Chapter 3

Microstructures, Dielectric Properties and Thermal Expansions of $Ba_{1-x}Sr_xTiO_3$ Solid Solution

3.1 Introduction

The properties of materials can be determined not only by the composition and structure but by their microstructure. The microstructure is usually characterized by optical microscope, SEM (scanning electron microscope) and TEM (transmission electron microscope). It can identify the number of phases including pores, shape and size distribution of grains which effect physical properties of ceramic products such as density, imperfection of crystal structure, mechanical and dielectric properties.

The solubility of TiO_2 in $BaTiO_3$ were studied by Sharma's group (4). They showed that the second phase was apparent at the triple point in the cases of Ba/Ti < 1.000. In addition, there was no second phase detected with a composition of Ba/Ti = 1.000, probably resulting from small variations in the accuracy of the preparation (17). For $BaTiO_3$ with excess BaO investigated by Hu's group (26), the second phase existed in the cases of Ba/Ti > 1.000.

In contrast to $BaTiO_3$, the micrographs of $SrTiO_3$ showed second phase particles for the sample having Sr/Ti = 1.000 (27).

In this research, microstructures for some compositions were characterized by SEM to determine the effects on density and dielectric properties.

The characteristics of dielectric ceramics are of increasing importance as the field of solid-state electronics continues expanding. The principal applications for these materials are as capacitive elements in electronic circuits and as electrical insulations. Thus, the dielectric properties such as the dielectric constant, dielectric loss and dielectric strength are the most concern. New devices and new applications are continually increasing the working range of frequency and the environmental conditions, particularly temperature, that are of partial interest. For applications as capacitors and electrical insulations, organic plastics are available: they are usually cheaper and can be fabricated with better dimensional accuracy than ceramics. The advantages of ceramics which frequently indicate their use, are superior electrical properties, absence of creep or deformation under stresses at room temperature and also greater resistance to environmental changes. All these factors have led to an increasing interest in dielectric ceramics.

One of the main advantages of ceramic dielectrics is that their loss factor is small compared with that of other available materials such as plastics. Energy losses in dielectrics result from three primary processes, ion migration, ion vibration and electron polarization. At room temperature, the loss factor is small at high frequencies. For a high capacitive material it is equally important to have a low value for the loss factor.

In general, a ceramic capacitor is desired to have a high capacitance with small dependences of electrostatic capacitance on the temperature and voltage. High capacitance material is found in a perovskite ceramic greatly used for electric power circuit. Although a high capacitance that a sharp peak of dielectric constant accompanying a phase transition is utilized, its disadvantage is the high dependence of dielectric constant on the temperature and electric field.

A diffuse phase transition or peak broadening is a way to lower the dependence of the dielectric constant on temperature. One method of peak broadening is to change the composition or form a solid solution encouraging random occupation of the same site with different cations.

Measurements are usually made as a function of temperature, frequency, dc-bias or pressure. In this study the purposes of these experiments were concerned with the change of dielectric constant and dissipation factor as a function of temperature and frequency.

The first aim was to investigate the transition temperature of $BaTiO_3$ and $Ba_{1-x}Sr_xTiO_3$ from room temperature to 200°C. From previous studies (17), BT was ferroelectric at room temperature and transformed to paraelectric above 125 ± 5°C. The maximum dielectric constant was about 10000 at Curie point. For BST, the transition temperature depended on amount of strontium. The compositions having less than 30 mol% of strontium were ferroelectric at room temperature and transformed to a paraelectric above room temperature (17).

In this study the dielectric constant and dissipation factor of $Ba_{1-x}Sr_xTiO_3$ were measured as a function of temperature and frequency. In addition, the phase transition temperature for each composition was determined from the dielectric data.

The specific volume of any given crystal increases with temperature, and the crystal tends to become more symmetrical. The change in volume due to lattice vibrations is closely related to the increase in energy content. Consequently, this results in the change of thermal expansion coefficient, $\alpha = \frac{1}{v}\left(\frac{dv}{dT}\right)$. For nonisometric

crystals, although the thermal expansion varies along different crystallographic axes, the result always gives a more symmetrical crystal at higher temperature. In tetragonal crystals of $BaTiO_3$, not only the c/a ratio but the expansion coefficients tended to decrease as the temperature increased (25).

In this experiment the linear thermal expansion of BST was used to determine the phase transition at which the slope was changed. The results of transition temperature would be compared to those from the dielectric data.

3.2 Procedure and Apparatus

3.2.1 Microstructure

The sintered samples were polished down to 1 μm by using sandpaper and diamond paste. Then polished samples were thermally etched at 100°C below sintering temperature and soaked at maximum temperature for 1 hr.

The microstructures of the selected samples were observed from the JEOL-JSM-5140LV Scanning Electron Microscope (SEM). In this experiment the effects of sintering temperature, soaking time and the amount of Sr dopant on the microstructure of $BaTiO_3$ would be studied.

3.2.2 Dielectric properties

The diameter and thickness of samples were measured by vernier calipers before electroding. Then both sides of samples were painted with silver paste as an electrode and fired at 700°C. The fired sample was put on the sample holder as shown in Fig. 3.1. A diagram of the apparatus is shown in Fig. 3.2. The capacitance and the dissipation factor were collected every 2°C with increasing temperature at 2°C/min from room temperature to 200°C. The measurements were made with HP

4192A LF Impedance Analyzer at different frequencies, 1, 10, 100 kHz and 1 MHz, respectively.

3.2.3 Thermal Expansion

The linear thermal expansion of sintered samples was characterized by NETZSCH Dilatometer. The data were collected from room temperature to 600°C with a heating rate 2°C/min.

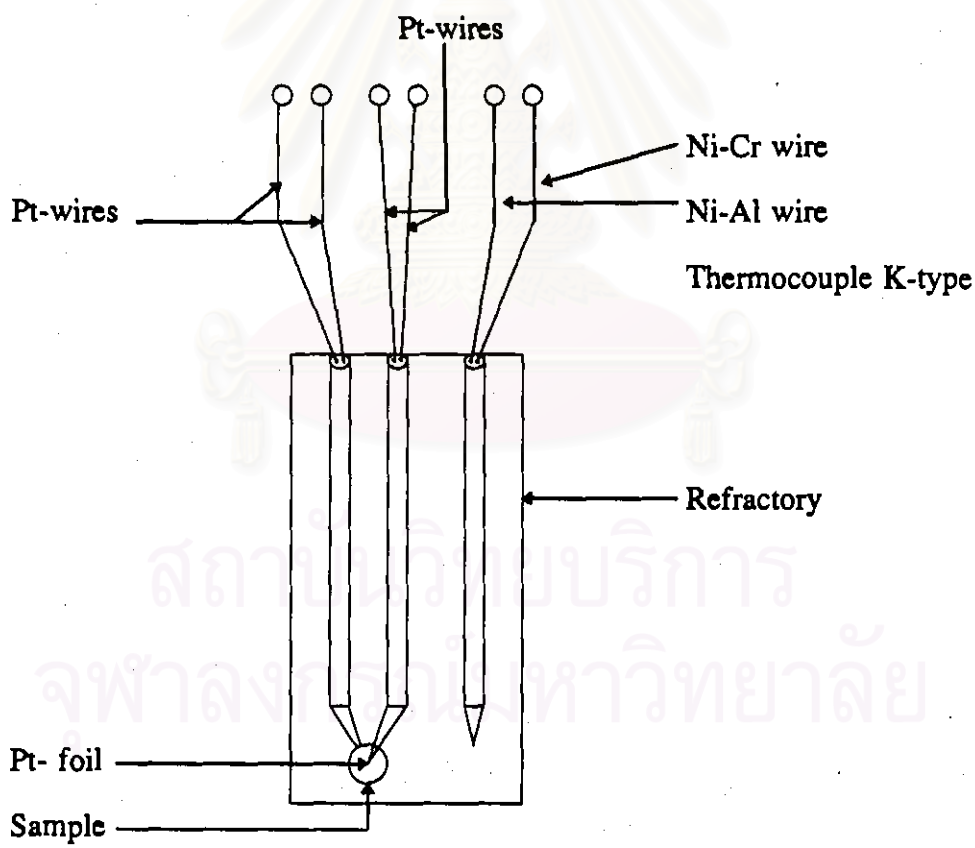

Fig. 3.1 Sample holder for the capacitance and dissipation factor measurement

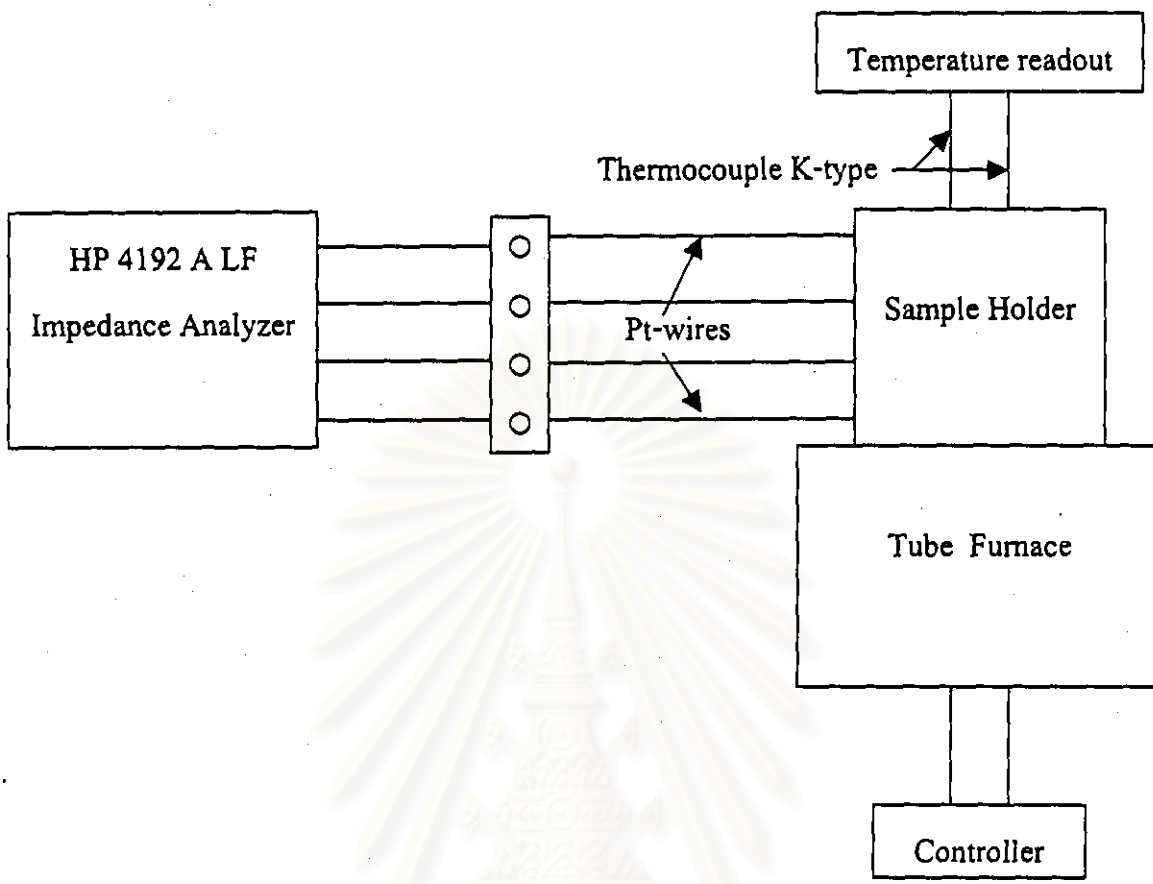

Fig. 3.2 Diagram of apparatus used for the capacitance and dissipation factor measurement at high temperature

3.3 Results and Discussion

3.3.1 Microstructure

Figures 3.3 (a) to (d) show the microstructure of $Ba_{1-x}Sr_xTiO_3$ with x=0, 0.1, 0.2 and 0.3, respectively. The effects of Sr^{2+} substitution to Ba^{2+} are compared for sintering temperature at 1400°C and soaked for 1 hr. Without Sr^{2+} the large grains of $BaTiO_3$ can be observed as shown in Fig.3.3 (a). An addition of 10 mol% of $SrTiO_3$ decreases the fraction of large grain significantly, resulting in a difference in grain size and thus increasing of pores occuring. In contrast, with 20 mol% $SrTiO_3$ addition (Fig.3.3(c)), a microstructure entirely consisting of uniform small grains is

obtained. Comparison of SEM micrographs in Fig. 3.3 shows that as the molar fraction of strontium increases from 0.0 to 0.3, the grain growth of $BaTiO_3$ is inhibited. These results are similar to the other works (8,17). The decreasing of grain size is argued that ionic radii of strontium are smaller than ionic radii of barium.

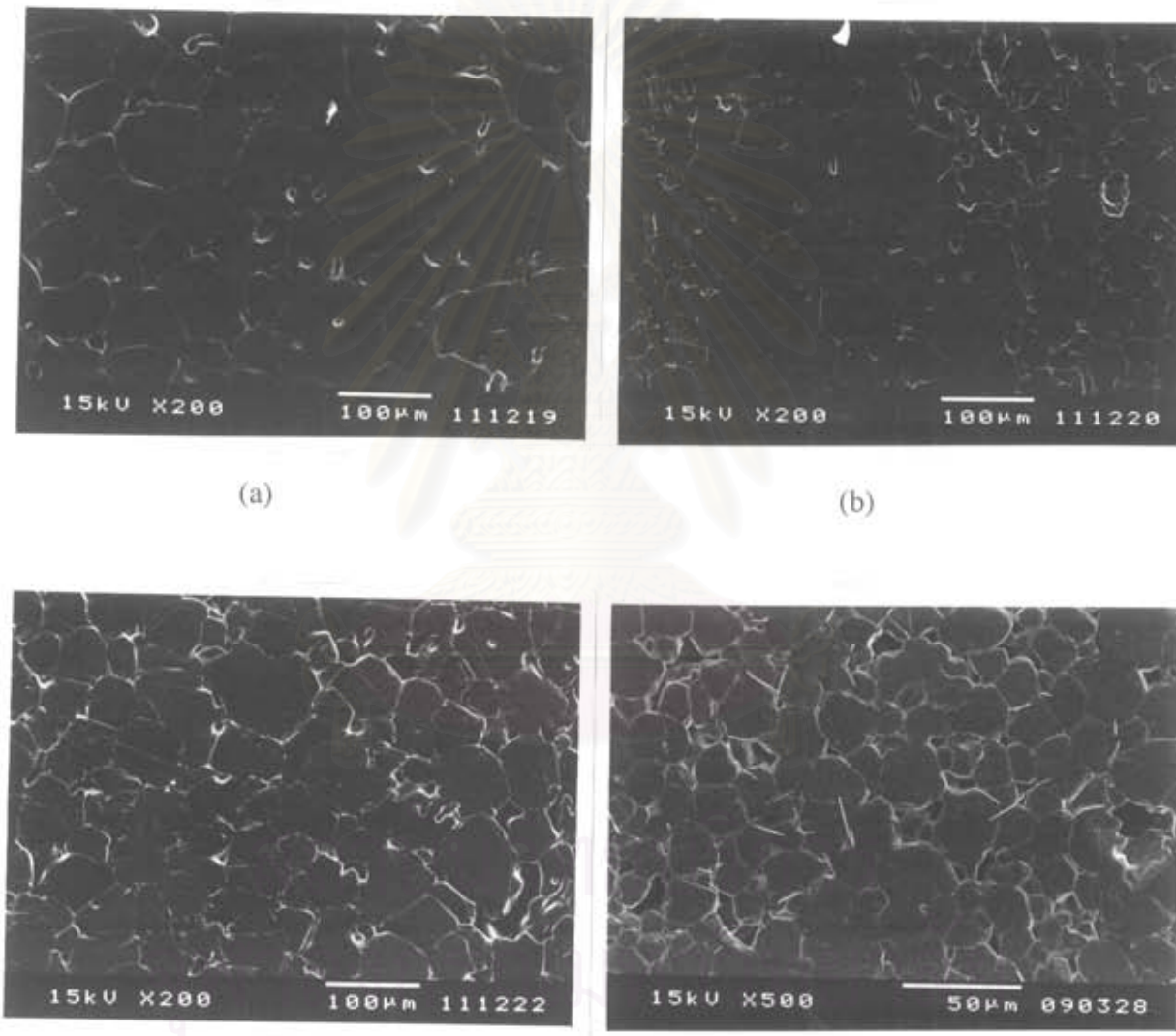

(a) (b)

(c) (d)

Fig.3.3 SEM micrographs of $Ba_{1-x}Sr_xTiO_3$ sintered at 1400°C and soaked for 1 hour. a) x=0 b) x= 0.1 c) x= 0.2 d) x=0.3

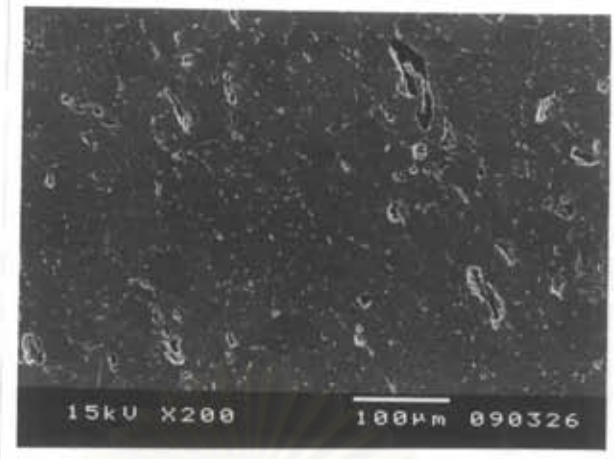

(a)

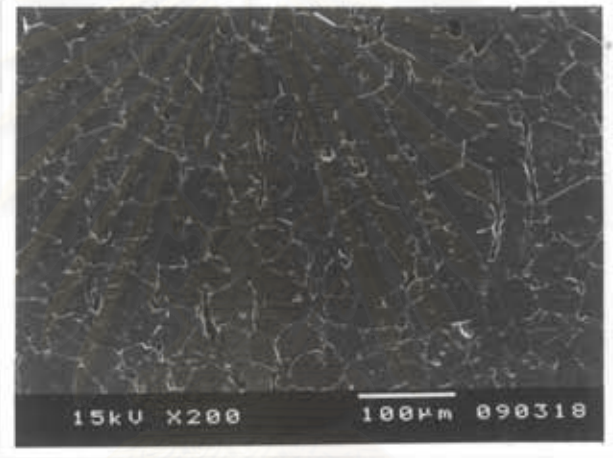

(b)

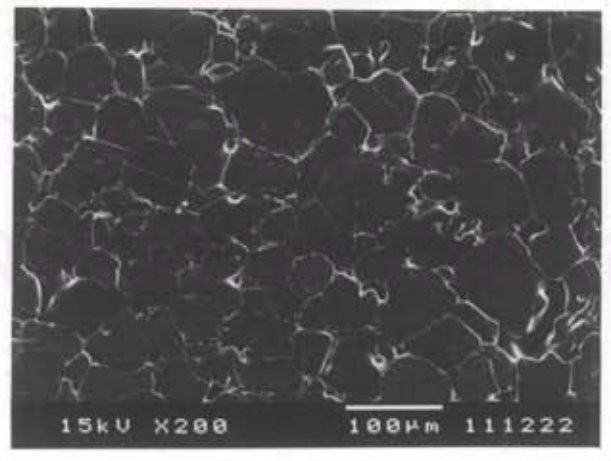

(c)

Fig.3.4 SEM micrographs of $Ba_{0.8}Sr_{0.2}TiO_3$ at different sintering temperature and holding for 1 hour. a) 1300°C b) 1350°C c) 1400°C

Fig. 3.4(a) to (c) show the progression of microstructural development as a function of sintering temperature from 1300°C to 1400°C and soaking time for 1 hr. The SEM micrographs show uniform grain sizes for all sintering temperatures, with larger grain sizes for the higher sintering temperature. Furthermore, the porosity decreases as the temperature increases.

Fig. 3.5(a) and (b) show the effect of soaking time on the microstructure of $Ba_{0.8}Sr_{0.2}TiO_3$ sintered at 1400°C. As soaking time increases from 30 minutes to 1 hour, the trend of grain size increases. The SEM micrographs show the decreasing of porosity and the distinguishable grain boundary as soaking time is increased.

In conclusion, from the results of SEM micrographs, the substitution of Sr to $BaTiO_3$ suppresses grain growth indicating decreasing of porosity. However, with an increasing amount of strontium the samples need to be sintered at a higher temperature.

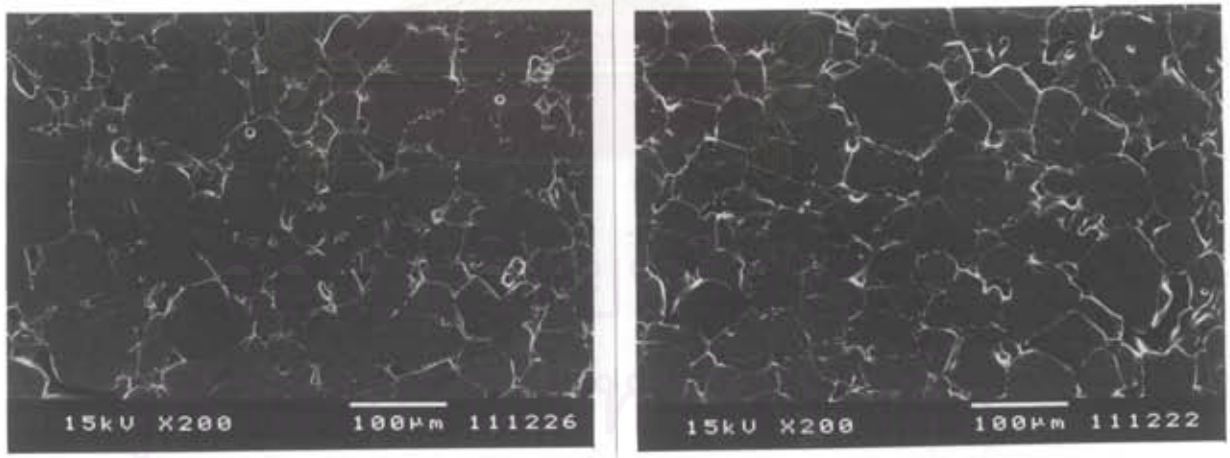

(a) (b)

Fig.3.5 SEM micrographs of $Ba_{0.8}Sr_{0.2}TiO_3$ sintered at 1400°C with different soaking time a) 30 minutes b) 1 hour.

3.3.2 Dielectric Constant and Dissipation Factor

The results of dielectric constant and dissipation factor as a function of temperature are shown in Fig. 3.6-3.12. Fig. 3.6 shows the dielectric constant and dissipation factor of $BaTiO_3$ sintered at 1300°C with soaking time for 30 minutes. The Curie point of this sample shows at 125°C and a maximum dielectric constant is about 10500. The frequency from 1 kHz to 1 MHz does not affect the dielectric constant. In other word, $BaTiO_3$ is not a relaxor since the dielectric constant is not depending on the frequency and the phase transition is not diffused. Below the Curie point the dielectric constant increases as the temperature increases. When the sample is heated from room temperature the interaction between Ti^{4+} ions and O^{2-} ions decreases, which increases the polarization. Above the Curie point the dielectric constant falls since the ferroelectric phase of $BaTiO_3$ has changed to a paraelectric phase.

Figure 3.6 shows the effects of frequency and temperature on dissipation factor of $BaTiO_3$. From room temperature, the dissipation factor decreases as the temperature increases for 1 kHz and 10 kHz. This is due to the domain wall motion in the ferroelectric region. At frequencies of 100 kHz and 1 MHz, the dissipation factor increases as the temperature increases since it increases the movement of domain wall. A hump of dissipation factor always occurs at the transition temperature of ferroelectric materials, which can be seen in Fig. 3.6 for $BaTiO_3$. Above the Curie point, the dissipation factor decreases because there is no domain wall in a paraelectric region. As the temperature is higher, the dissipation factor tends to increase due to the effect of conductivity. It increases significantly if the measurement is taken at a low frequency.

The results of Fig. 3.7 indicate that the Curie temperature is independent of the sintering temperature. The Curie temperatures of $BaTiO_3$ sintered at different temperatures are about 126°C-128°C. However, it affects the dielectric constant and the dissipation factor of $BaTiO_3$. The dielectric constant increases as the sintering temperature increases as shown in Fig 3.8.

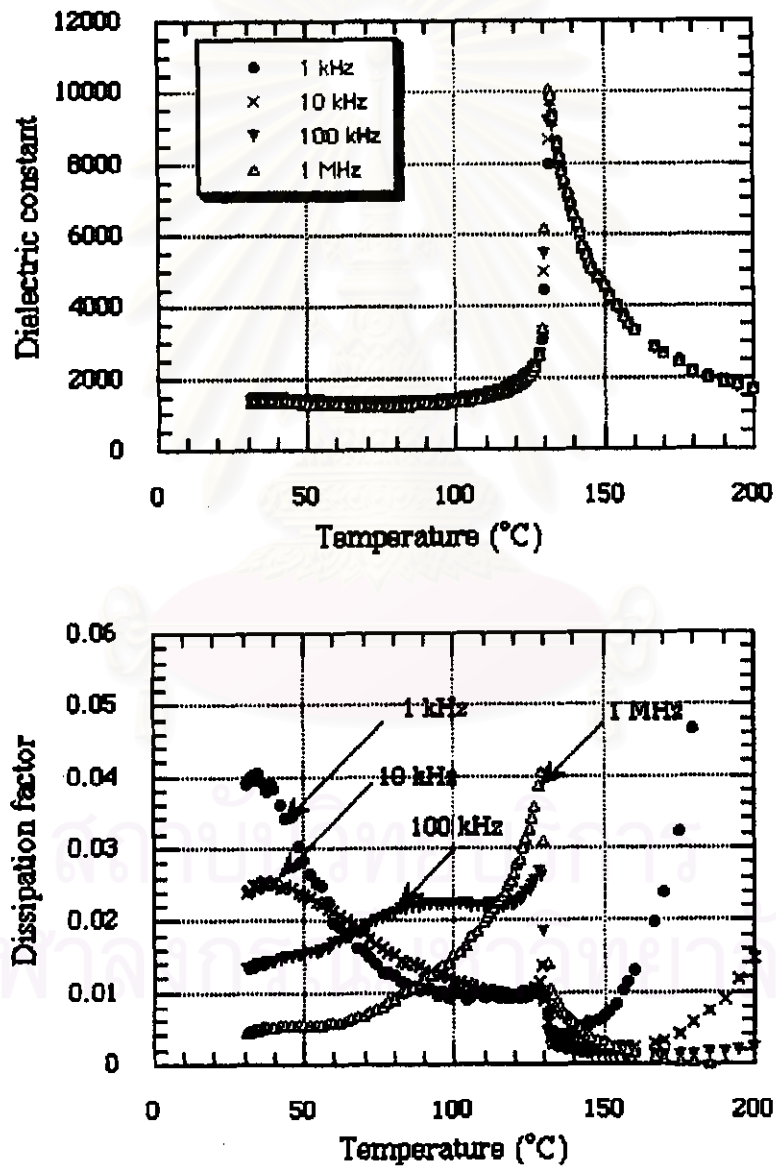

Fig. 3.6 Change in dielectric constant and dissipation factor at different frequencies of $BaTiO_3$ sintered at 1300°C and soaked for 30 minutes.

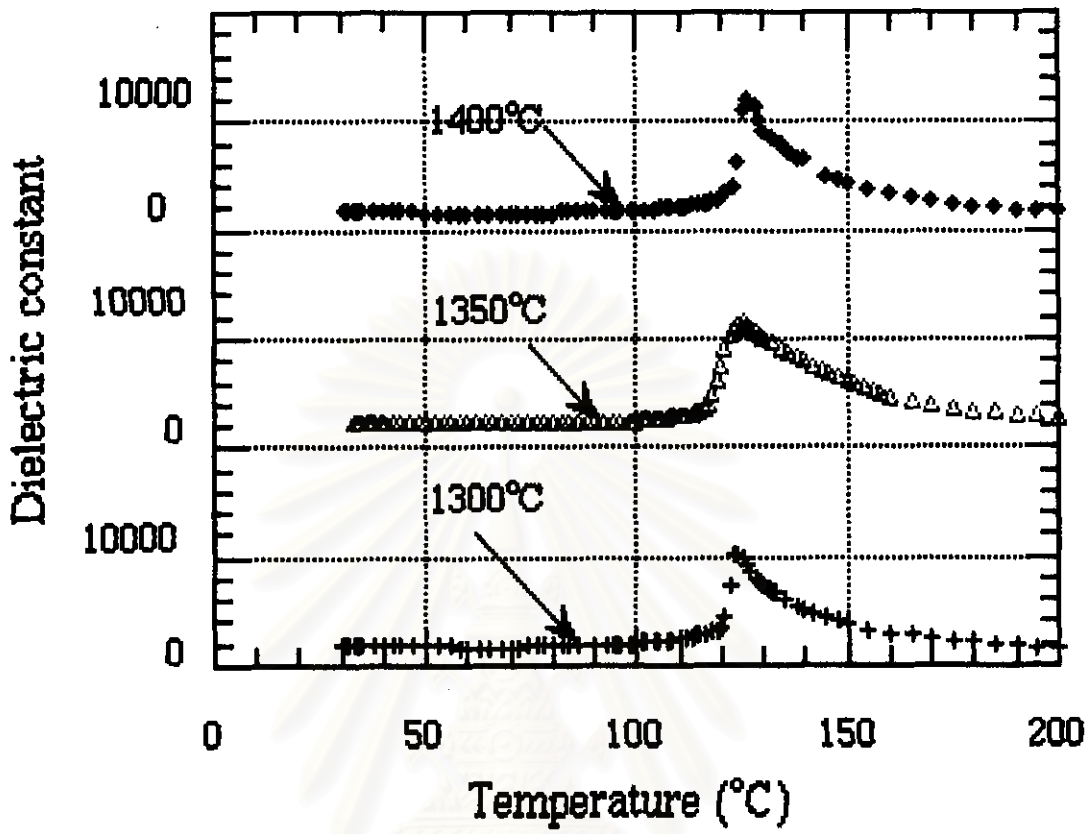

Fig. 3.7 Change in dielectric constant of $BaTiO_3$ at different sintering temperature.

The effect of soaking time on the dielectric constant and dissipation factor of $BaTiO_3$ sintered at 1400°C is shown in Fig. 3.9. The dielectric constants of $BaTiO_3$ with soaking for 30 minutes are closed to those for 1 hour for all measurement temperature, which show no effect of soaking time on the dielectric constant. The dissipation factor of $BaTiO_3$ with soaking for 30 minutes has a higher value than that for 1 hour but the differential value is so small. The results indicate that the soaking time has a small effect on dielectric properties. However, there is a tendency of a lower dissipation factor for the composition with a longer soaking time due to elimination of pores. In addition, the difference of the soaking time in this work is only 30 minutes, which may not be long enough to compare.

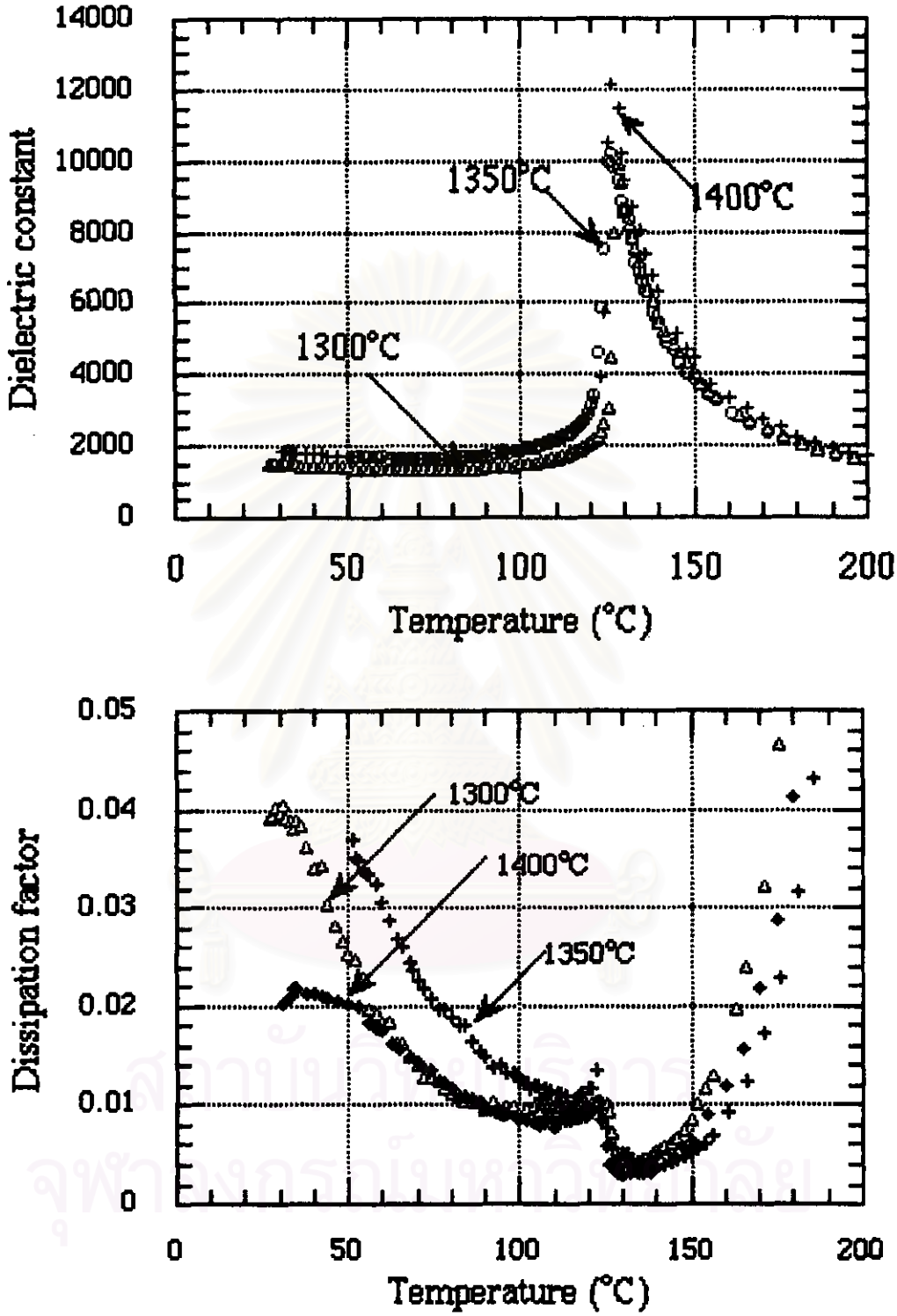

Fig. 3.8 Change in dielectric constant and dissipation factor of $BaTiO_3$ at different sintering temperature and soaked for 30 minutes at a frequency of 10 kHz.

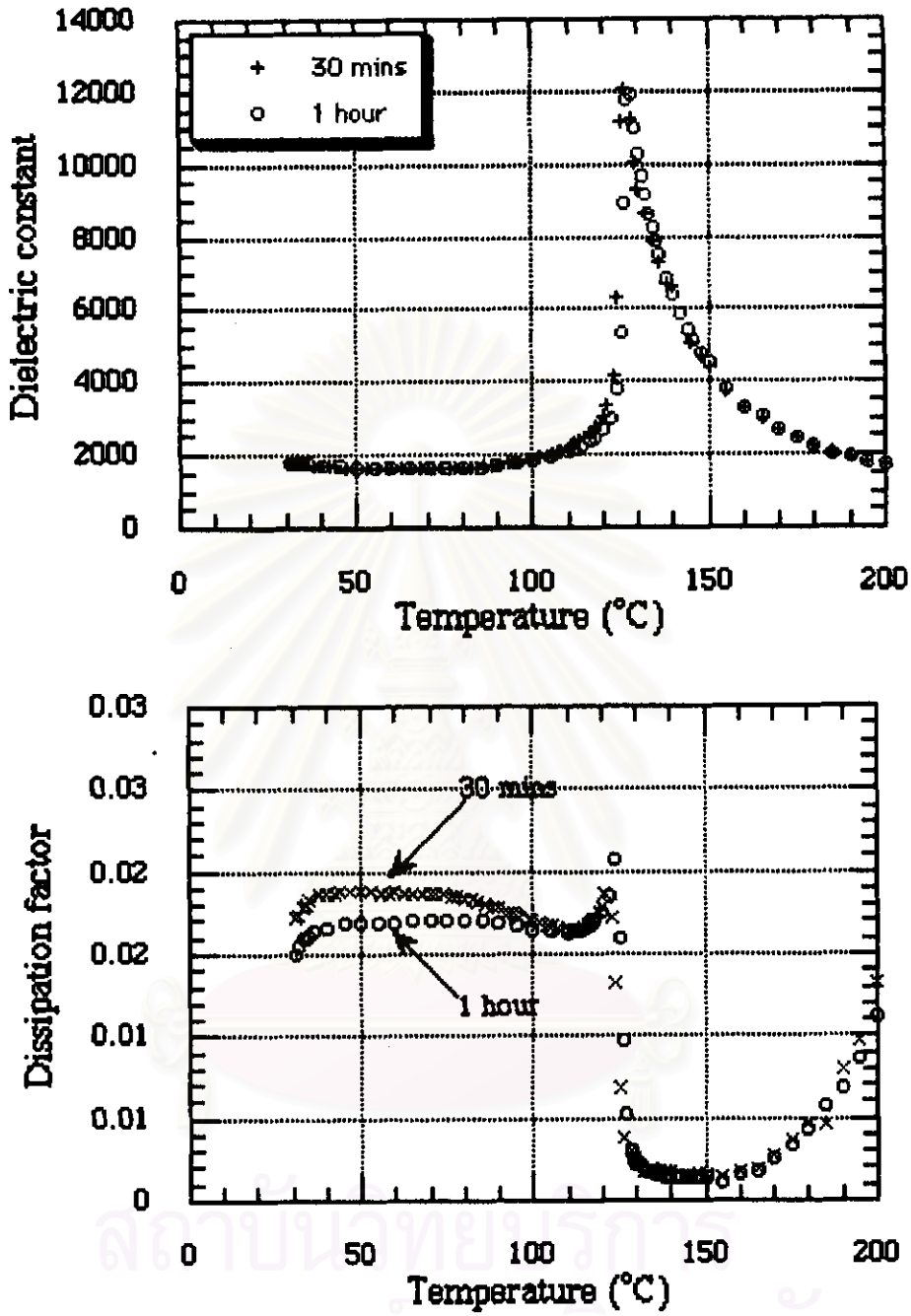

Fig. 3.9 Change in dielectric constant and dissipation factor of $BaTiO_3$ at different soaking time at a frequency measurement of 10 kHz.

The effects of Sr^{2+} on the dielectric constant and the dissipation factor of $BaTiO_3$ are shown in Fig. 3.10 and 3.11. Fig. 3.10 shows the dielectric constant and the dissipation factor of $Ba_{1-x}Sr_xTiO_3$ ($0 \leq x \leq 0.3$) sintered at 1350°C and soaked for

30 minutes at a frequency measurement of 10 kHz. As the molar fraction of strontium increases, the Curie point is lowered and also broadening. The Curie temperature of $BaTiO_3$ decreases from 124°C to 97°C with an addition of Sr (x=0.1). When x is changed to 0.2 and 0.3, the Curie temperature appears at 63°C and 32°C, respectively.

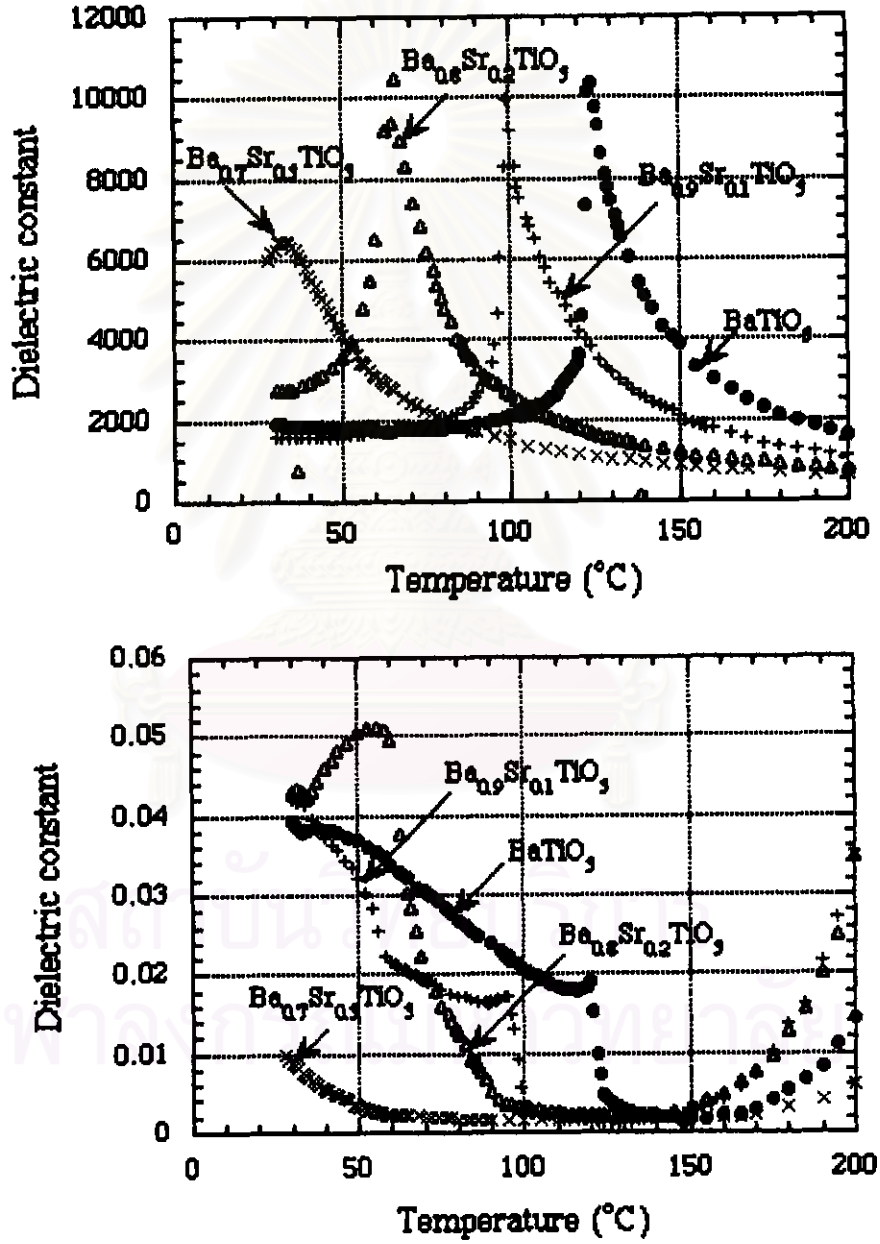

Fig. 3.10 Change in dielectric constant and dissipation factor of $Ba_{1-x}Sr_xTiO_3$ system at sintering temperature of 1350°C

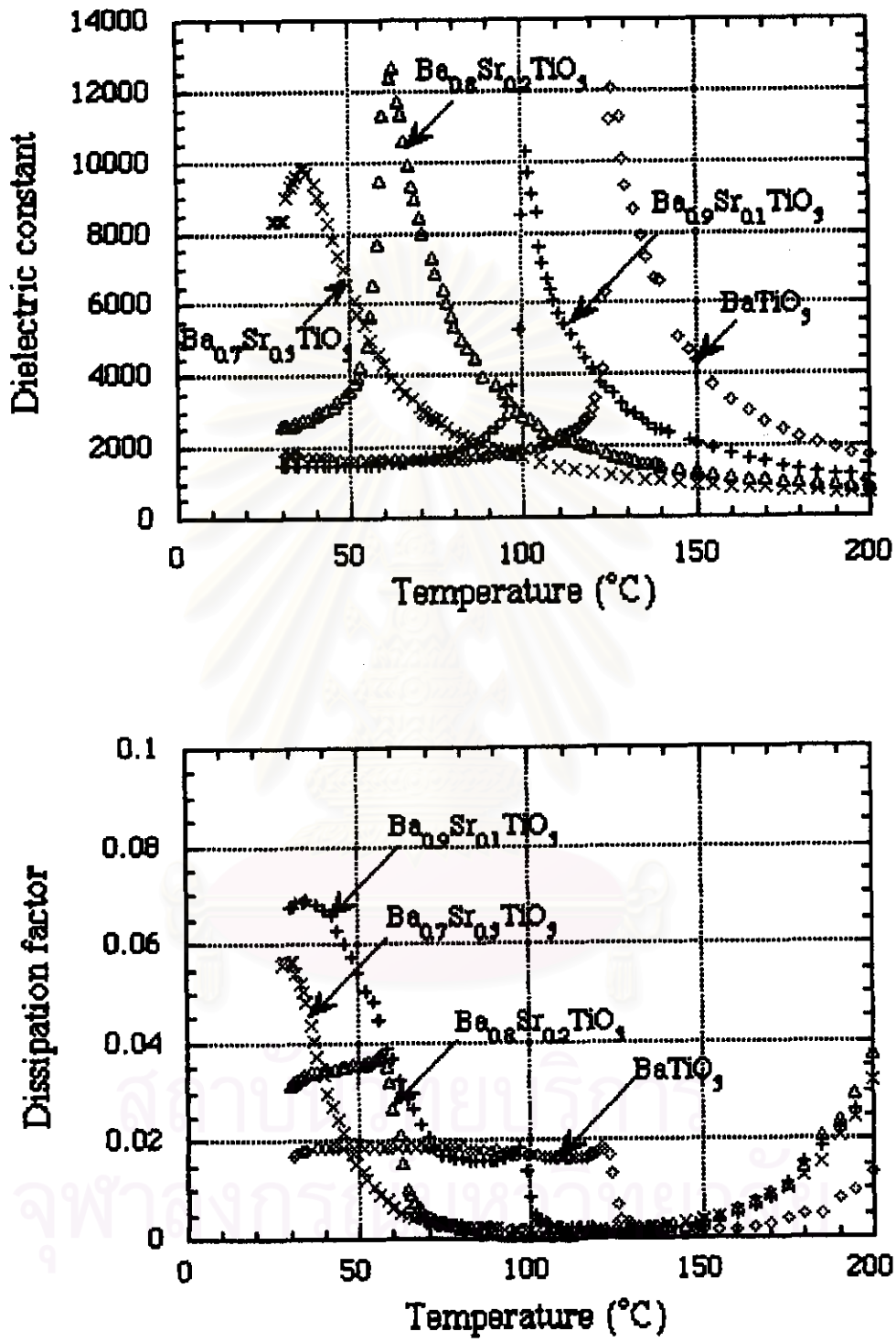

Fig. 3.11 Change in dielectric constant and dissipation factor of $Ba_{1-x}Sr_xTiO_3$ system at sintering temperature of 1400°C.

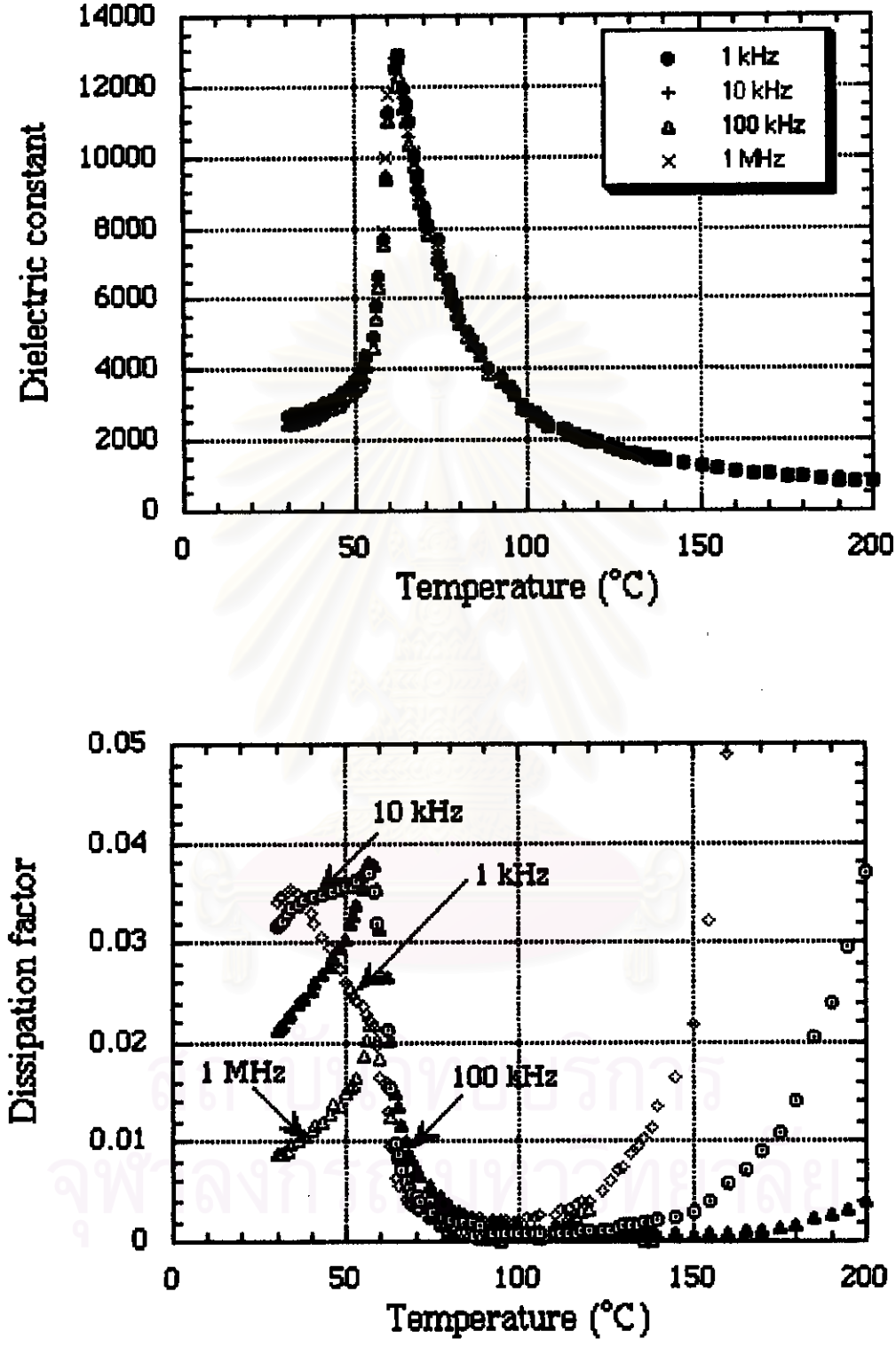

Fig. 3.12 Change in dielectric constant and dissipation factor at different frequencies of $Ba_{0.8}Sr_{0.2}TiO_3$ sintered at 1400°C.

The trend of dielectric constant increases as x increases up to 0.3. This is probably due to the high dielectric constant of Sr expected from $SrTiO_3$ and the smaller grain size. In addition, the uniform grain size distribution, less porosity and surface imperfection are affected. The dielectric constant decreases as x=0.3. This result indicates a larger amount of pores in this composition as compared to the others illustrated in Fig. 3.3. These results are similar to Liou's work (17) and Bunting's work (18). The dissipation factor for all BST in this research is similar but the turning points are different and dependence on the amount of strontium. The results of dissipation factor go along with those of dielectric constant. When the sintering temperature increases, the trend of dielectric constant values increases for all compositions as compared Fig 3.11 to Fig 3.10, due to the lower porosity, which is confirmed by SEM micrograph of $Ba_{0.8}Sr_{0.2}TiO_3$ in Fig. 3.4. The Curie temperatures for $Ba_{1-x}Sr_xTiO_3$ are 126°C, 97°C, 63°C and 35°C for x=0, 0.1, 0.2 and 0.3, respectively. This also implies that the sintering temperature does not affect the Curie point of the same composition.

The results of maximum dielectric constant and the transition temperature as a function of composition, sintering temperature and soaking time are summarized in Table 4-7. The tolerance of the Curie temperature is about 2-3°C because of the distribution of temperature in a furnace and the position of thermocouple.

From the results of dielectric data for $Ba_{0.8}Sr_{0.2}TiO_3$ in Fig 3.12, its maximum dielectric constant is about 13000. This graph indicates that measurement frequencies are very small dependence on dielectric constant, assuming that there is no effect on dielectric constant. However, the frequency clearly affects the dissipation factor below the transition temperature since the applied frequency gives the distribution to the movement of domain wall.

The dielectric properties of $Ba_{0.8}Sr_{0.2}TiO_3$ samples with different sintering conditions are investigated. The results show the same responses or the same shapes but the values of dielectric constant increase at a higher sintering temperature. In general, the higher sintering temperature and longer soaking time increase the grian size, which results in reducing the dielectric constant of $BaTiO_3$. However, in this experiment, the maximum dielectric constant increases as the sintering temperature increases. The probable reason may come from other factor such as higher density or less pores which is predominant effect.

The results of microstructure and dielectric constant are considered for the best selected composition that gives a uniform microstructure and higher dielectric constant. Thus, the composition of $Ba_{0.8}Sr_{0.2}TiO_3$ is selected to be base material for further study with other dopants such as Pb, Ca and Zr in the following chapter.

Table 4 Maximum dielectric constant and Curie temperature for $Ba_{1-x}Sr_xTiO_3$ as a function of composition and sintering temperature at a frequency of 1 kHz.

1300°C

composition	Maximum k'	Curie temperature (°C)
$BaTiO_3$	9920	125
$Ba_{0.9}Sr_{0.1}TiO_3$	7635	95
$Ba_{0.8}Sr_{0.2}TiO_3$	7696	62
$Ba_{0.7}Sr_{0.3}TiO_3$	5150	33

1350°C

composition	Maximum k'	Curie temperature (°C)
$BaTiO_3$	10189	126
$Ba_{0.9}Sr_{0.1}TiO_3$	9866	96
$Ba_{0.8}Sr_{0.2}TiO_3$	10496	60
$Ba_{0.7}Sr_{0.3}TiO_3$	6661	34

1400°C

composition	Maximum k'	Curie temperature (°C)
$BaTiO_3$	12075	128
$Ba_{0.9}Sr_{0.1}TiO_3$	11687	95
$Ba_{0.8}Sr_{0.2}TiO_3$	13316	62
$Ba_{0.7}Sr_{0.3}TiO_3$	11469	33

Table 5 Maximum dielectric constant and Curie temperature for $Ba_{1-x}Sr_xTiO_3$ as a function of frequency and composition sintered at 1300°C.

$BaTiO_3$

Frequency (kHz)	30 minutes		1 hour	
	Maximum k'	Curie temperature	Maximum k'	Curie temperature
1	9920	125	10538	125
10	9785	125	10481	125
100	9635	125	10456	125
1000	9918	125	10915	125

$Ba_{0.9}Sr_{0.1}TiO_3$

Frequency (kHz)	30 minutes		1 hour	
	Maximum k'	Curie temperature	Maximum k'	Curie temperature
1	7636	95	10349	95
10	7547	95	10226	95
100	7547	95	10099	95
1000	7450	95	10661	95

$Ba_{0.8}Sr_{0.2}TiO_3$

Frequency (kHz)	30 minutes		1 hour	
	Maximum k'	Curie temperature	Maximum k'	Curie temperature
1	7969	62	12169	62
10	7870	62	11899	62
100	7698	62	11605	62
1000	7940	62	12201	62

$Ba_{0.7}Sr_{0.3}TiO_3$

Frequency (kHz)	30 minutes		1 hour	
	Maximum k'	Curie temperature	Maximum k'	Curie temperature
1	5151	34	5011	34
10	4913	34	4808	34
100	4713	34	4615	34
1000	4729	34	4624	34

Table 6 Maximum dielectric constant and Curie temperature for $Ba_{1-x}Sr_xTiO_3$ as a function of frequency and composition sintered at 1350°C.

$BaTiO_3$

Frequency (kHz)	30 minutes		1 hour	
	Maximum k'	Curie temperature	Maximum k'	Curie temperature
1	10469	124	10189	126
10	10329	124	10092	126
100	10188	124	9965	126
1000	10487	124	10316	126

$Ba_{0.9}Sr_{0.1}TiO_3$

Frequency (kHz)	30 minutes		1 hour	
	Maximum k'	Curie temperature	Maximum k'	Curie temperature
1	10032	97	9866	96
10	9984	97	9588	96
100	9926	97	9210	96
1000	10194	97	9252	96

$Ba_{0.8}Sr_{0.2}TiO_3$

Frequency (kHz)	30 minutes		1 hour	
	Maximum k'	Curie temperature	Maximum k'	Curie temperature
1	10805	63	10496	60
10	10457	63	10319	60
100	9838	63	10269	60
1000	9913	63	10541	60

$Ba_{0.7}Sr_{0.3}TiO_3$

Frequency (kHz)	30 minutes		1 hour	
	Maximum k'	Curie temperature	Maximum k'	Curie temperature
1	6557	32	6661	34
10	6472	32	6513	34
100	6412	32	6422	34
1000	6607	32	6532	34

Table 7 Maximum dielectric constant and Curie temperature for $Ba_{1-x}Sr_xTiO_3$ as a function of frequency and composition sintered at 1400°C.

$BaTiO_3$

Frequency (kHz)	30 minutes		1 hour	
	Maximum k'	Curie temperature	Maximum k'	Curie temperature
1	12161	126	12075	128
10	12059	126	11889	128
100	11870	126	11700	128
1000	12539	126	12371	128

$Ba_{0.9}Sr_{0.1}TiO_3$

Frequency (kHz)	30 minutes		1 hour	
	Maximum k'	Curie temperature	Maximum k'	Curie temperature
1	10305	97	11687	95
10	10279	97	11611	95
100	10157	97	11505	95
1000	10639	97	12296	95

$Ba_{0.8}Sr_{0.2}TiO_3$

Frequency (kHz)	30 minutes		1 hour	
	Maximum k'	Curie temperature	Maximum k'	Curie temperature
1	12894	63	13316	62
10	12667	63	13070	62
100	12297	63	12683	62
1000	12855	63	13211	62

$Ba_{0.7}Sr_{0.3}TiO_3$

Frequency (kHz)	30 minutes		1 hour	
	Maximum k'	Curie temperature	Maximum k'	Curie temperature
1	10642	35	11469	33
10	9829	35	10995	33
100	9406	35	10735	33
1000	9743	35	11274	33

3.3.3 Thermal Expansion of $Ba_{1-x}Sr_xTiO_3$ crystal

The results of thermal expansion for $Ba_{1-x}Sr_xTiO_3$ where x=0, 0.1, 0.2 and 0.3 at different sintering temperatures are shown in Fig. 3.13 and those at different soaking times are shown in Fig. 3.14.

The results of thermal expansion can identify the isotropic-anisotropic structure by the slope changing (25). Fig. 3.15-3.17 show the thermal expansion coefficient of $Ba_{1-x}Sr_xTiO_3$ (x=0, 0.1, 0.2 and 0.3) sintered at 1300°C, 1350°C and 1400°C, respectively, for 30 minutes soaking time. An increasing of Sr content can lower the phase transition temperature of $BaTiO_3$, which can be seen from the inflection point about 115°C-123°C for undoped $BaTiO_3$, 90°C-95°C for x = 0.1, 55°C-60°C for x = 0.2 and 30°C-32°C for x = 0.3. The results are similar to the results from the dielectric data but the phase transition temperatures between these two methods are different, approximately 2-8°C, depending on the position of thermocouple. The trend of thermal expansion coefficient above Curie point increases as the amount of Sr increases, as shown in Fig 3.13-3.14 and summarized in Table 8. The thermal expansion coefficient at Curie point of $BaTiO_3$ which sintered at 1300°C and soaked for 30 minutes is about $-20*10^{-6}/°C$ and reduced to $-13*10^{-6}/°C$, $-10*10^{-6}/°C$ and $-9*10^{-6}/°C$, for x= 0.1. 0.2 and 0.3, respectively. The results show that $BaTiO_3$ has the highest anisotropic structure and $Ba_{0.7}Sr_{0.3}TiO_3$ has the lowest anisotropic structure. In other word, Sr reduces the C.O.E. of $BaTiO_3$ the room temperature to the Curie point. These data confirm the results of lattice parameters calculated from XRD pattern illustrating the decreasing of nonisometric crystals or c/a ratio as Sr increases.

In conclusion, the effect of Sr-dopant on transition temperature of $BaTiO_3$ has much more significance than that of sintering temperature and soaking time. The

greater amount of Sr in $BaTiO_3$, the lower of the Curie temperature. The phase transition temperature from C.O.E. results are different from dielectric properties because the positions of thermocouple in each apparatus are different.

Table 8 The transition temperature as a function of composition , sintering temperature and soaking time

1300°C for 30 minutes

composition	phase transition temperature	C.O.E. above T_c ($*10^{-6}/1/^{\circ}C$)
$BaTiO_3$	122.8	8.0
$Ba_{0.9}Sr_{0.1}TiO_3$	94.4	8.2
$Ba_{0.8}Sr_{0.2}TiO_3$	62.4	8.5
$Ba_{0.7}Sr_{0.3}TiO_3$	30.9	8.9

1350°C for 30 minutes

composition	phase transition temperature	C.O.E. above T_c ($*10^{-6}/1/^{\circ}C$)
$BaTiO_3$	115.1	8.0
$Ba_{0.9}Sr_{0.1}TiO_3$	91.0	8.3
$Ba_{0.8}Sr_{0.2}TiO_3$	53.3	8.2
$Ba_{0.7}Sr_{0.3}TiO_3$	30.9	8.2

1400°C

composition	phase transition temperature		C.O.E. above T_c ($*10^{-6}/1/^{\circ}C$)	
	30 minutes	1 hour	30 minutes	1 hour
$BaTiO_3$	115.6	117.1	7.3	8.1
$Ba_{0.9}Sr_{0.1}TiO_3$	90.6	93.0	8.4	8.1
$Ba_{0.8}Sr_{0.2}TiO_3$	55.8	57.6	8.5	8.3
$Ba_{0.7}Sr_{0.3}TiO_3$	31.9	32.5	8.5	8.5

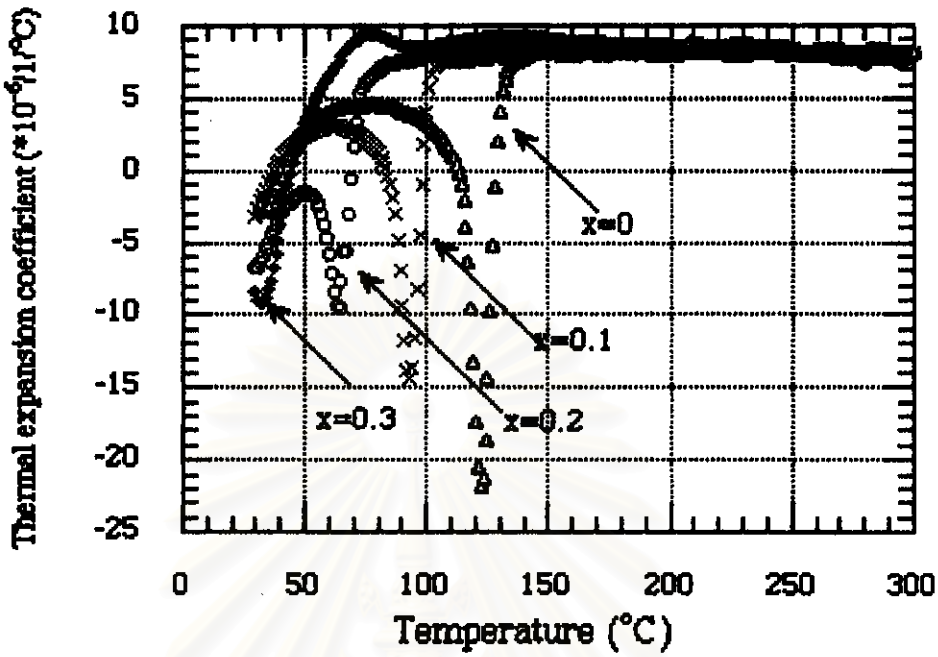

(a)

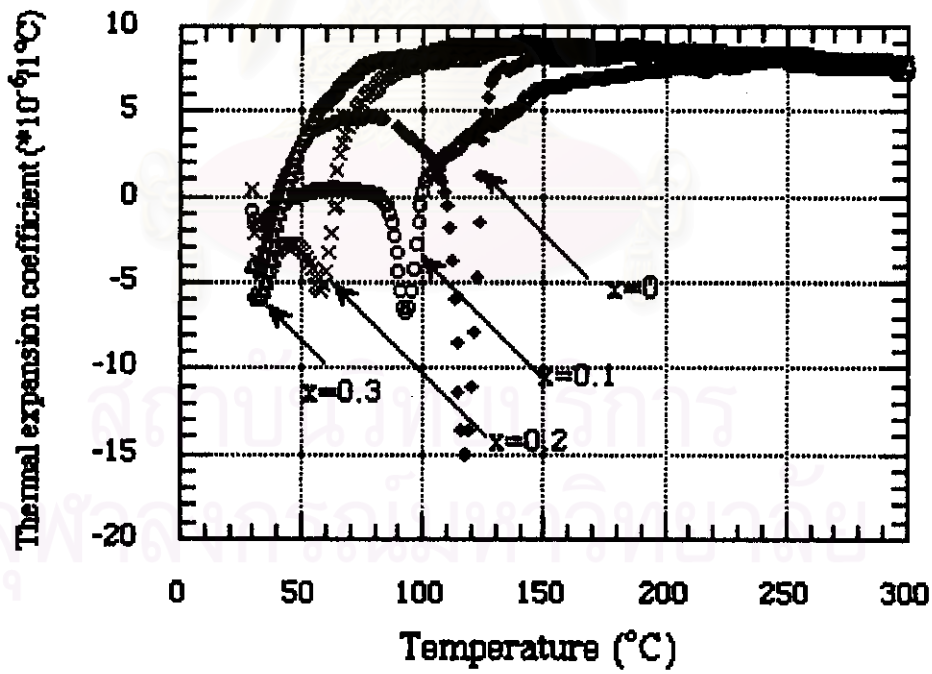

(b)

Fig. 3.13 Change in thermal expansion coefficient of $Ba_{1-x}Sr_xTiO_3$ at different sintering temperatures and soaking time for 1 hour.

(a) 1300°C (b) 1400°C

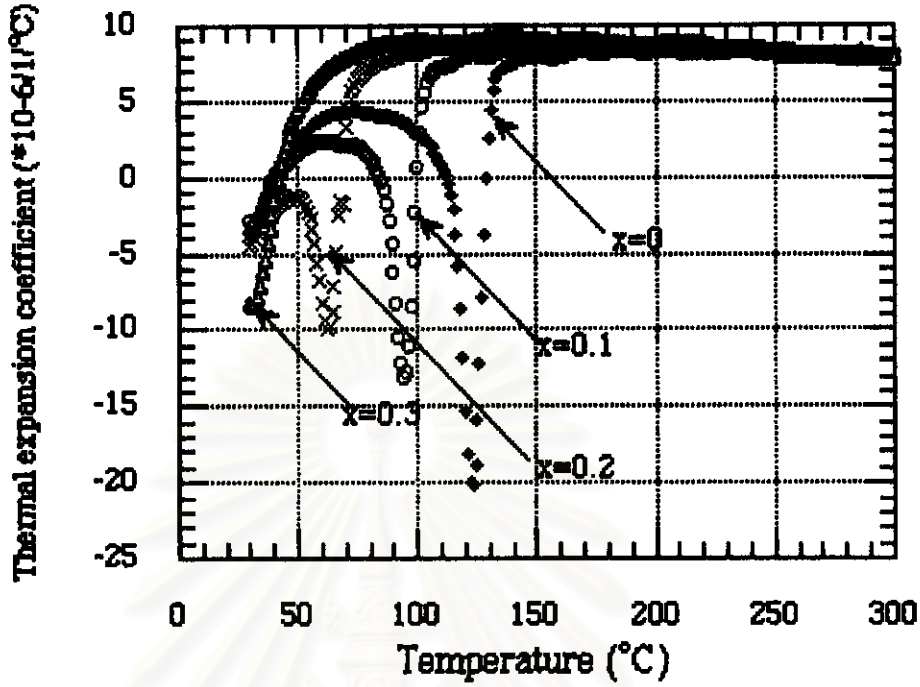

(a)

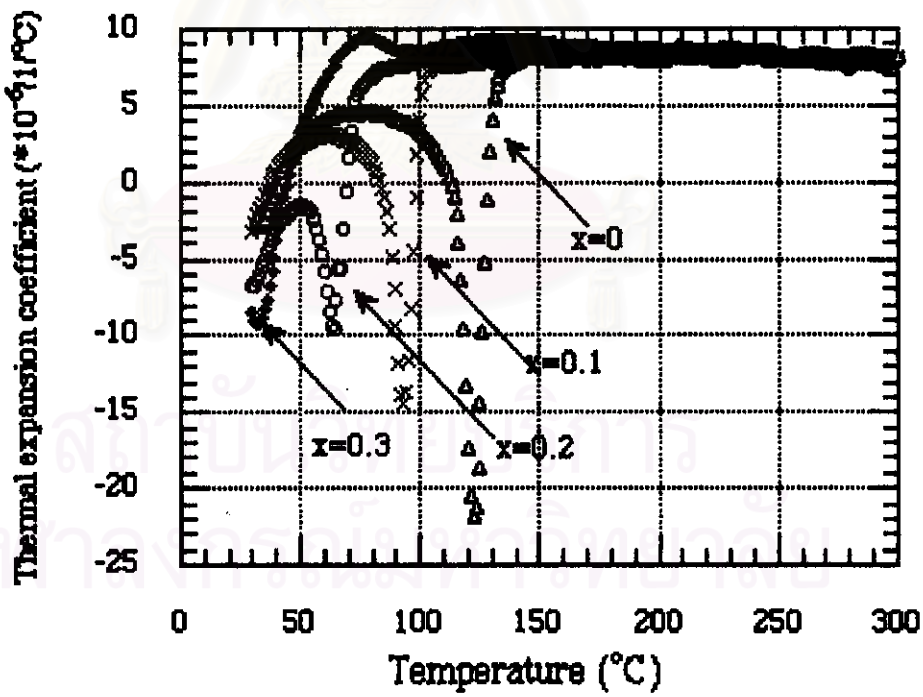

(b)

Fig. 3.14 Change in thermal expansion coefficient of $Ba_{1-x}Sr_xTiO_3$ sintered at 1300°C with different soaking times.

(a) 30 minutes (b) 1 hour

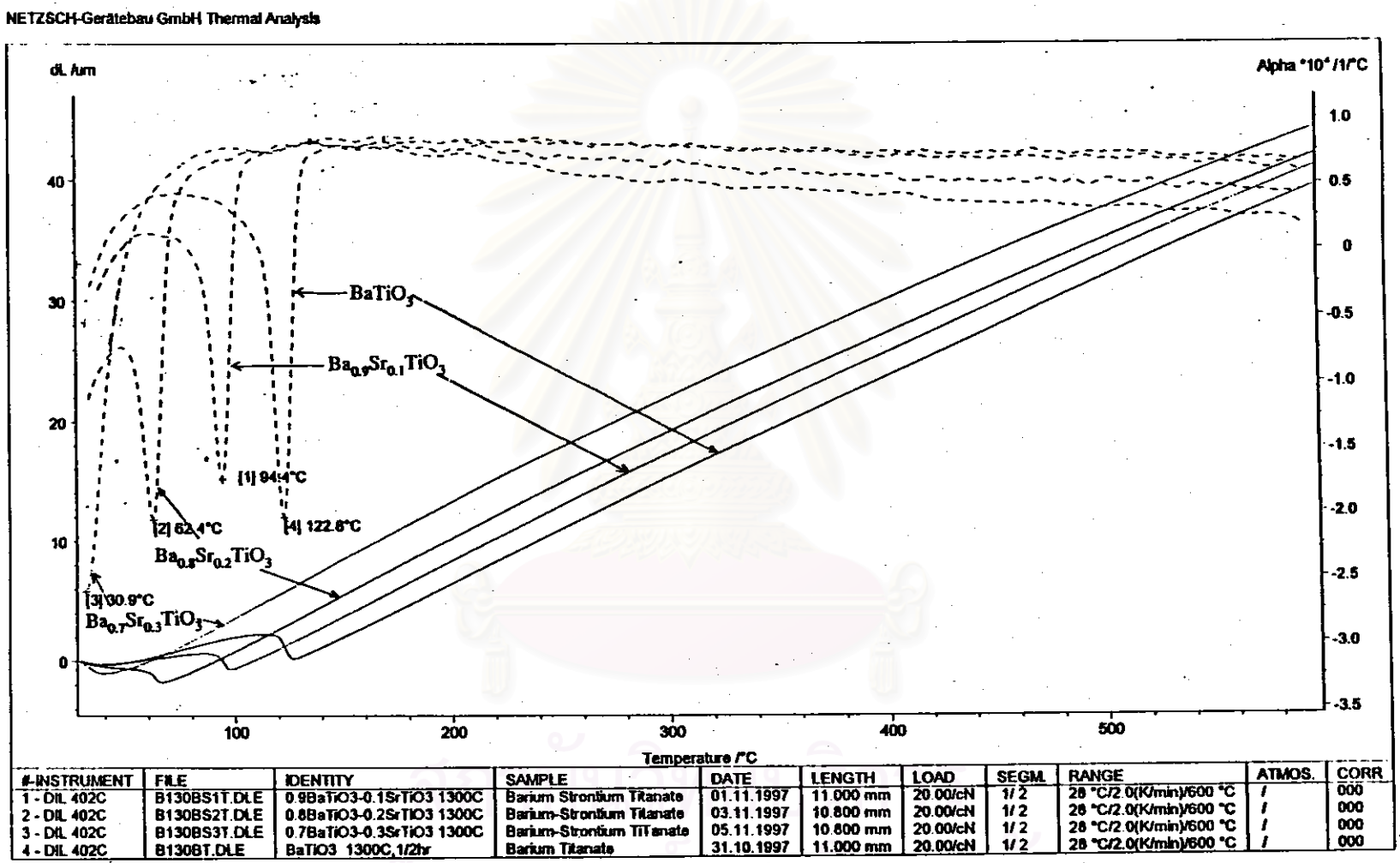

#-INSTRUMENT	FILE	IDENTITY	SAMPLE	DATE	LENGTH	LOAD	SEGM.	RANGE	ATMOS.	CORR
1 - DIL 402C	B130BS1T.DLE	0.9BaTiO3-0.1SrTiO3 1300C	Barium Strontium Titanate	01.11.1997	11.000 mm	20.00/cN	1/ 2	28 °C/2.0(K/min)/600 °C	/	000
2 - DIL 402C	B130BS2T.DLE	0.8BaTiO3-0.2SrTiO3 1300C	Barium-Strontium Titanate	03.11.1997	10.800 mm	20.00/cN	1/ 2	28 °C/2.0(K/min)/600 °C	/	000
3 - DIL 402C	B130BS3T.DLE	0.7BaTiO3-0.3SrTiO3 1300C	Barium-Strontium TiTanate	05.11.1997	10.600 mm	20.00/cN	1/ 2	28 °C/2.0(K/min)/600 °C	/	000
4 - DIL 402C	B130BT.DLE	BaTiO3 1300C,1/2hr	Barium Titanate	31.10.1997	11.000 mm	20.00/cN	1/ 2	28 °C/2.0(K/min)/600 °C	/	000

Fig. 3.15 Change in linear shrinkage and thermal expansion coefficient of $Ba_{1-x}Sr_xTiO_3$ sintered at 1300°C with 30 minutes soaking

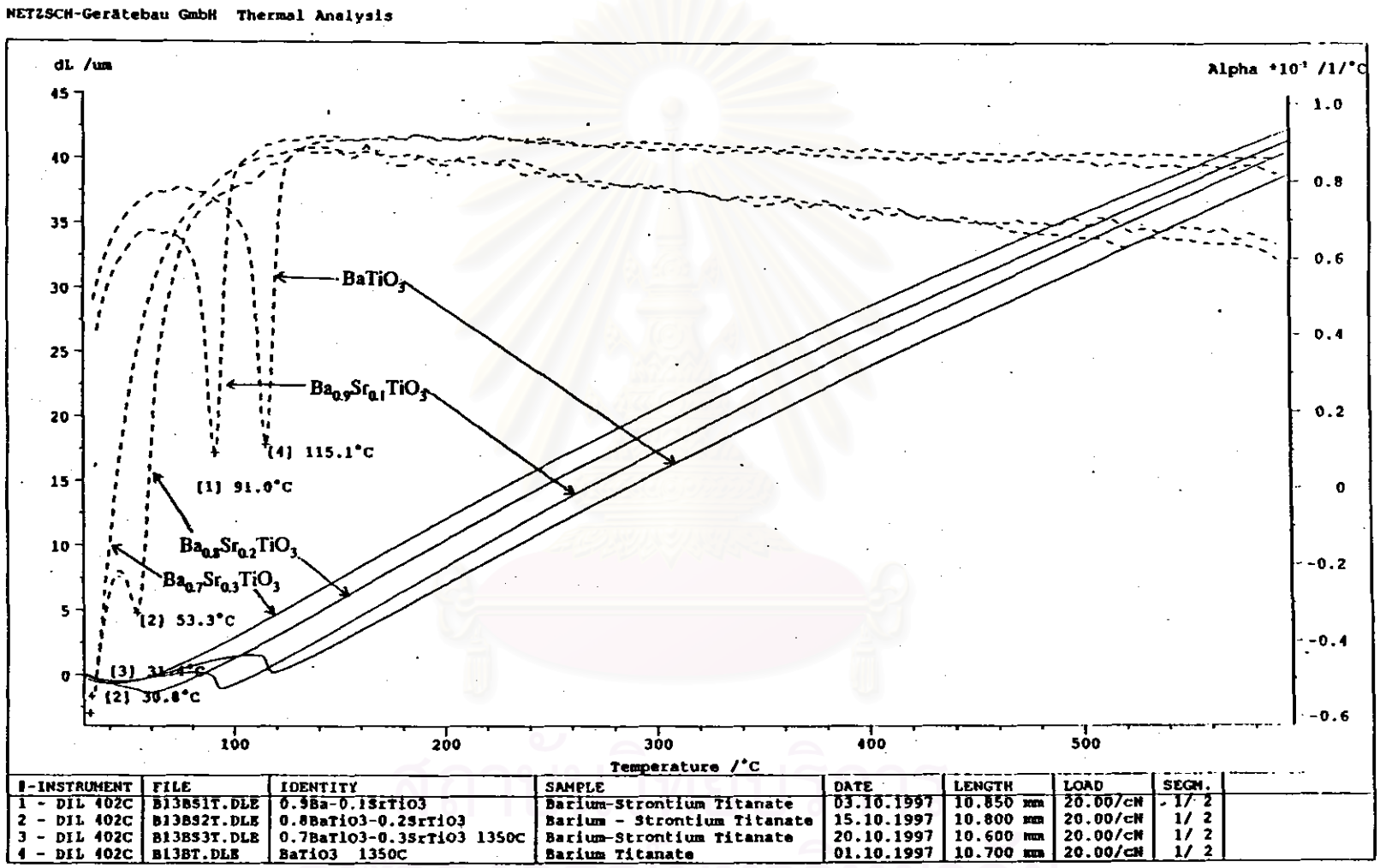

Fig. 3.16 Change in linear shrinkage and thermal expansion coefficient of $Ba_{1-x}Sr_xTiO_3$ sintered at 1350°C with 30 minutes soaking

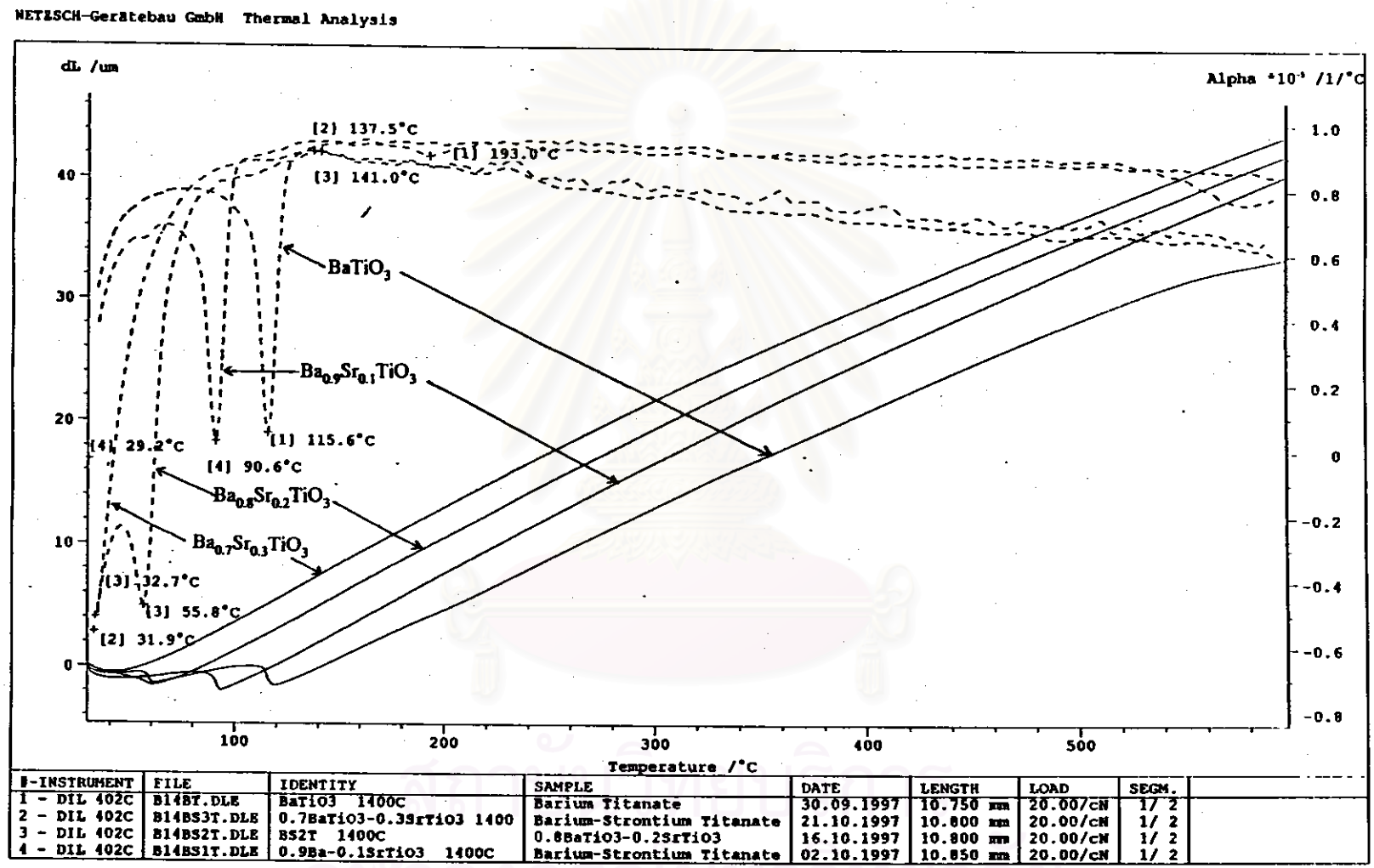

Fig. 3.17 Change in linear shrinkage and thermal expansion coefficient of $Ba_{1-x}Sr_xTiO_3$ sintered at 1400°C with 30 minutes soaking